Immune targeting of mycobacteria through cell surface glycan engineering

Priscilla Dzigba,[a,b,c] Adrian K. Rylski,[a] Isaac J. Angera,[a] Nicholas Banahene,[a,c] Herbert W. Kavunja,[a] Mallary C. Greenlee-Wacker[b,d]* and Benjamin M. Swarts[a,c,]*

[a]Department of Chemistry and Biochemistry and [b]Department of Biology, Central Michigan University, Mount Pleasant, MI, 48859, USA

[c]Biochemistry, Cell, and Molecular Biology Graduate Programs, Central Michigan University, Mount Pleasant, MI, 48859 United States

[d]Biological Sciences Department, California Polytechnic State University, San Luis Obispo, CA, 93407, USA

*Corresponding author: E-mail: ben.swarts@cmich.edu

*Corresponding author: E-mail: mcgreenl@calpoly.edu

Abstract

Mycobacteria and other organisms in the Mycobacteriales order cause a range of significant human diseases, including tuberculosis, leprosy, diphtheria, Buruli ulcer, and non-tuberculous mycobacterial (NTM) disease. However, the intrinsic drug tolerance engendered by the mycobacterial cell envelope undermines conventional antibiotic treatment and contributes to acquired drug resistance. Motivated by the need to augment antibiotics with novel therapeutic approaches, we developed a strategy to specifically decorate mycobacterial cell surface glycans with antibody-recruiting molecules (ARMs), which flag bacteria for binding to human-endogenous antibodies that enhance macrophage effector functions. Mycobacteria-specific ARMs consisting of a trehalose targeting moiety and a dinitrophenyl hapten (Tre-DNPs) were synthesized and shown to specifically incorporate into outer membrane glycolipids of *Mycobacterium smegmatis* via trehalose metabolism, enabling recruitment of anti-DNP antibodies to the mycobacterial cell surface. Phagocytosis of Tre-DNP-modified *M. smegmatis* by macrophages was significantly enhanced in the presence of anti-DNP antibodies, demonstrating proof-of-concept that our strategy can augment the host immune response. Because the metabolic pathways responsible for cell surface incorporation of Tre-DNPs are conserved in all Mycobacteriales organisms but absent from other bacteria and humans, the reported tools may be enlisted to interrogate host-pathogen interactions and develop immune-targeting strategies for diverse mycobacterial pathogens.

Introduction

Mycobacterial pathogens are characterized by a distinctive dual-membrane cell envelope that provides extraordinary protection from antibiotics and is a major driver of acquired drug resistance. The most prominent example of these organisms is *Mycobacterium tuberculosis*, which every year causes approximately 10 million cases of active tuberculosis (TB) and 1.6 million deaths, making it the world's leading cause of death by a bacterial pathogen.[1,2] Due to intrinsic drug tolerance provided by the mycobacterial cell envelope, conventional treatment of *M. tuberculosis* infections requires the administration of multiple drugs over the course of 6 months.[3,4] The long duration, intensiveness, and side effects associated with this treatment regimen curb its effectiveness and have ultimately contributed to the emergence of multi-drug resistant (MDR)-TB, which is extremely challenging and expensive to treat.[4,5] Other mycobacterial infections are similarly recalcitrant to treatment with antibiotics. Non-tuberculous mycobacteria (NTM), such as *M. avium* and *M. abscessus*, are ubiquitous and represent an increasingly common cause of severe pulmonary disease, particularly in immunocompromised individuals (e.g., patients with cystic fibrosis or HIV).[6,7] Treatment of NTM infection involves a complicated 12-month combinatorial drug regimen that is often ineffective and can lead to the acquisition of resistance mutations.[8,9] Leprosy, diphtheria, and Buruli ulcer, which are also caused by mycobacteria or closely related corynebacteria, also present challenges with respect to chemotherapy and drug resistance.[10] Given the inherent difficulty of treating mycobacterial infections with existing antibiotics, the rise and spread of strains with accumulated antibiotic resistance mutations, and the paucity of new anti-mycobacterial compounds in the drug pipeline, there is a need for novel therapeutic approaches that complement traditional antibiotics.[11,12]

Host-directed immunotherapies represent an attractive target for novel anti-mycobacterial treatments.[13–16] A robust cell-mediated immune response is needed to eliminate *M. tuberculosis* from their intracellular niche within the macrophage, as well as to foster the development of interferon-γ-producing T cells that maintain granuloma structure during latent tuberculosis.[17] Likewise, protective immune response to pulmonary NTM include macrophage killing and T cell-dependent cytokine production.[18] Given the well-established role of cellular effector functions, but despite evidence showing that antibodies are protective in most cases,[19] the potential role of antibodies in mycobacterial infections has been underappreciated until recently. To address whether antibodies played a protective role in mycobacterial infections, Watson and colleagues recently showed that a

monoclonal antibody directed against *M. tuberculosis* phosphate transporter subunit PstS1 increased mycobacterial uptake by a macrophage cell line, decreased bacterial numbers, and improved survival in mice.[20] Antibody ligation of Fc-receptors and subsequent Fc-receptor signaling is a likely driver of this protective response because antibody-targeting of *M. bovis*, as well as other intracellular bacteria, to Fc-receptors increases lysosome fusion and restricts intracellular growth in phagocytes.[20–25] Together, these data support the notion that antibodies, which target mycobacterial surface molecules and enhance phagocytosis, might be a successful immunotherapy.

On the basis that Fc-mediated phagocytosis enhances phagocytosis and killing of other intracellular pathogens,[23,25] we hypothesized that specific cell surface engineering of mycobacterial glycans with antibody-recruiting small molecules (ARMs) would enhance antibody-dependent phagocytosis by macrophages. ARMs are rationally designed to contain a pathogen-targeting motif and an antibody recruitment motif, the latter of which is recognized by naturally occurring antibodies to trigger macrophage effector functions.[26–30] In order to overcome developing drug resistance, as well as immune evasion caused by natural variation in surface antigens, the selection of the pathogen-targeting motif can also be tailored to select essential surface molecules where mutations would be lethal. The ARM concept has previously been applied to create immunotherapy strategies for cancer,[31–34] viruses,[35] fungi,[36] and various types of bacteria, including *Escherichia coli*, *Helicobacter pylori*, *Enterococcus faecium* and *Staphylococcus aureus*.[37–42] Here, we report proof-of-concept for the first mycobacteria-targeting ARM immunotherapy strategy. We demonstrate that novel ARMs consisting of trehalose as the mycobacteria-targeting motif and dinitrophenyl (DNP) as the antibody-recruiting motif specifically modify cell surface glycans of the model organism *M. smegmatis*, enabling bacterium-targeted anti-DNP antibody binding and enhancement of phagocytosis by macrophages. This work provides a platform for investigating antibody-mediated immune responses to mycobacterial infections and sets the stage for the development of immunotherapy strategies directed against diverse mycobacterial pathogens.

Results and Discussion

Design and synthesis of Tre-DNP analogues as mycobacteria-targeting ARMs. As first-generation ARMs, we envisioned trehalose–DNP conjugates whose trehalose and DNP components serve as the mycobacteria-targeting and antibody-recruiting elements, respectively (Figure 1). DNP is attractive in ARM

development because approximately 1% of antibodies in humans bind to nitroarene epitopes such as DNP, and 72% of the general population has endogenous anti-DNP antibodies.[43,44] In addition, DNP is relatively small and synthetically tractable, which we anticipated would aide in cell surface incorporation and structural optimization efforts. To achieve specific delivery of DNP to the mycobacterial surface, potentially even within complex host settings, we chose to exploit trehalose metabolic pathways that are present and conserved in mycobacteria but absent from other bacteria and humans.[45] All mycobacteria have a complex cell envelope consisting of several layers, including plasma membrane, peptidoglycan, arabinogalactan, and the mycobacterial outer membrane (Figure 1A).[46] An essential and abundant component of the outer membrane is the non-mammalian disaccharide trehalose, which exists in lipidated forms referred to as trehalose mono- and dimycolate (TMM and TDM). We and others have shown that trehalose and TMM analogues containing various functional groups (e.g., bioorthogonal tags, fluorophores) on the sugar or lipid portions can be efficiently metabolically incorporated into outer membrane glycans, including TMM and TDM, via mycoloyltransferase activity (for incorporation mechanism, see Scheme S1, Supporting Information).[47–56] Furthermore, we have demonstrated that trehalose and TMM analogues do not modify canonical Gram-positive and Gram-negative bacteria, supporting their specificity for mycobacteria.[49,55]

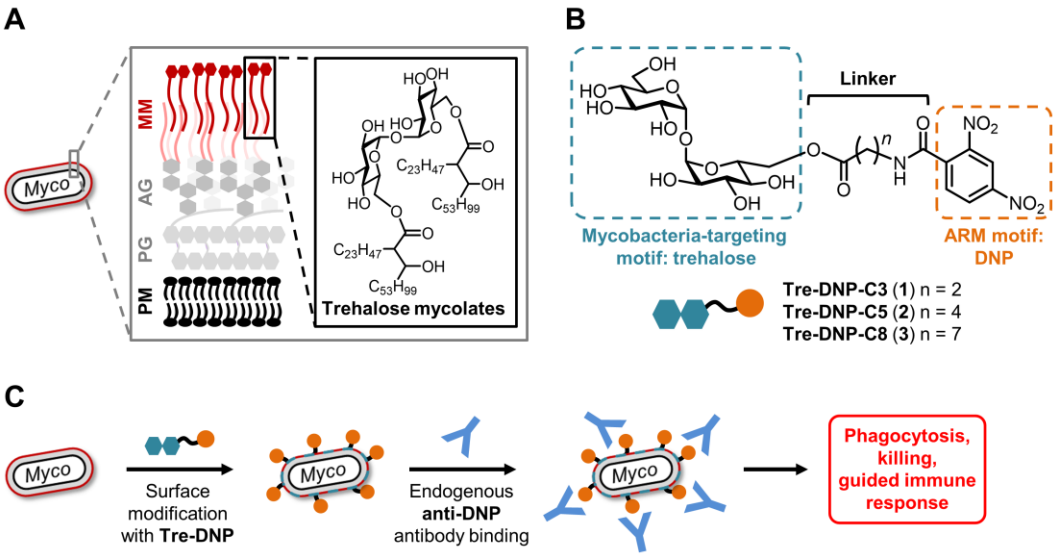

Figure 1. (A) Trehalose mycolates are exposed at the surface of the mycobacterial cell envelope. (B) Tre-DNP analogues are mycobacteria-specific ARMs developed in this study. (C) Tre-DNP-based ARM immune-targeting strategy for mycobacteria.

Based on the above considerations, we designed DNP-modified trehalose (Tre-DNP) analogues **1**–**3** as

ARMs with ester-connected linkers of variable length (Figure 1B). The synthesis of the target Tre-DNP analogues was accomplished by adapting Kulkarni's approach to the preparation of trehalose monoesters (Scheme 1).[56] First, the N-hydroxysuccinimide ester of 2,4-dinitrobenzoic acid[57] (DNP-OSu, **4**) was conjugated to amino acids of differing length, providing the appropriate DNP-modified carboxylic acids in 60–95% yield (**5**–**7**). Compounds **5**–**7** were also utilized in metabolic incorporation experiments as control compounds lacking the trehalose targeting group. Subsequently, intermediates **5**–**7** were used in the 6-*O*-monoesterification of trimethylsilyl (TMS)-protected trehalose diol **8** in the presence of *N,N'*-dicyclohexylcarbodiimide (DCC) and 4-dimethylaminopyridine (DMAP). Following desilylation with Dowex H^+ resin in methanol, the target compounds (**1**–**3**) were obtained in 17–32% yield over two steps, which is in line with previously reported syntheses of trehalose monoesters.[49,51,55] We also developed an alternative synthesis of Tre-DNP analogues involving late-stage installation of the DNP group onto a trehalose intermediate with an amine-functionalized linker, which should provide improved versatility for accessing related ARMs in the future (Scheme S2, Supporting Information).

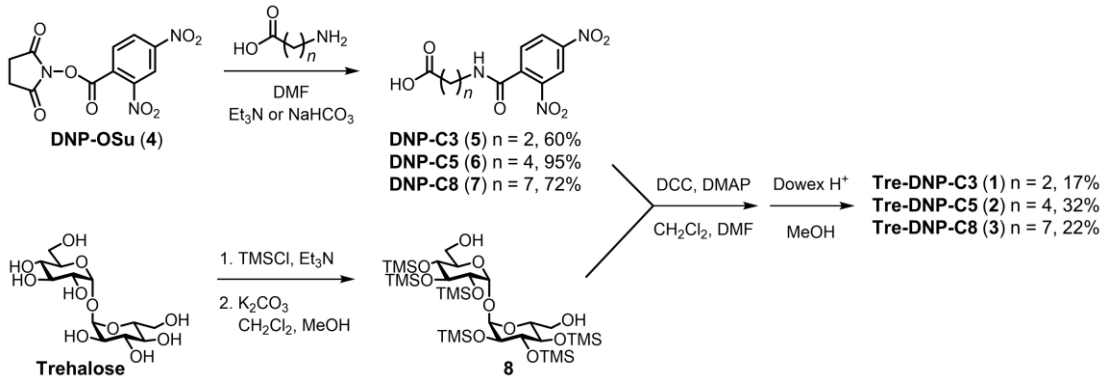

Scheme 1. Chemical synthesis of Tre-DNP analogues **1**–**3** and DNP-carboxylic acids **5**–**7**.

Tre-DNP analogues specifically incorporate into the cell surface of mycobacteria. With the target Tre-DNP analogues in hand, we evaluated their incorporation into mycobacterial cells. For this proof-of-concept study, we utilized the fast-growing, non-pathogenic mycobacterial species *M. smegmatis* as a model organism. To determine which linker length promoted the most efficient incorporation of DNP into the cell surface, wild-type *M. smegmatis* mc^2155 was incubated in compounds **1**–**3** at varying concentrations or left untreated, stained with a commercial anti-DNP-keyhole limpet hemocyanin (KLH) antibody conjugated to Alexa Fluor 488, and analyzed

by flow cytometry. DNP-carboxylic acids **5**–**7** were tested in parallel as control compounds lacking the trehalose targeting component. Each Tre-DNP analogue incorporated into *M. smegmatis* in a dose-dependent manner, whereas no incorporation of the corresponding DNP-carboxylic acids was observed, suggesting that the incorporation of Tre-DNPs **1**–**3** was specific and driven by trehalose metabolism (Figure 2A). Of the three Tre-DNP compounds, Tre-DNP-C8 (**3**), with the longest linker, was incorporated and detected with the highest efficiency. This could be a result of more efficient metabolic incorporation, improved accessibility of the surface-displayed DNP to the anti-DNP antibody, or a combination thereof. The results were consistent with our previous study on alkyne-containing trehalose analogues, which showed that an analogue containing a 7-carbon chain was metabolically incorporated and detected by click chemistry more efficiently than compounds with 5- and 11-carbon chains.[49] An isotype control antibody did not bind to Tre-DNP-C8-labeled *M. smegmatis*, confirming the specificity of the anti-DNP antibody fluorescence signal for surface-accessible DNP groups (Figure 2B). Imaging of Tre-DNP-C8-labeled cells showed that fluorescence signal was localized to the bacterial surface and poles (Figure 2C), which is consistent with the polar growth mode of mycobacteria and with published imaging experiments employing trehalose-based probes.[49,55]

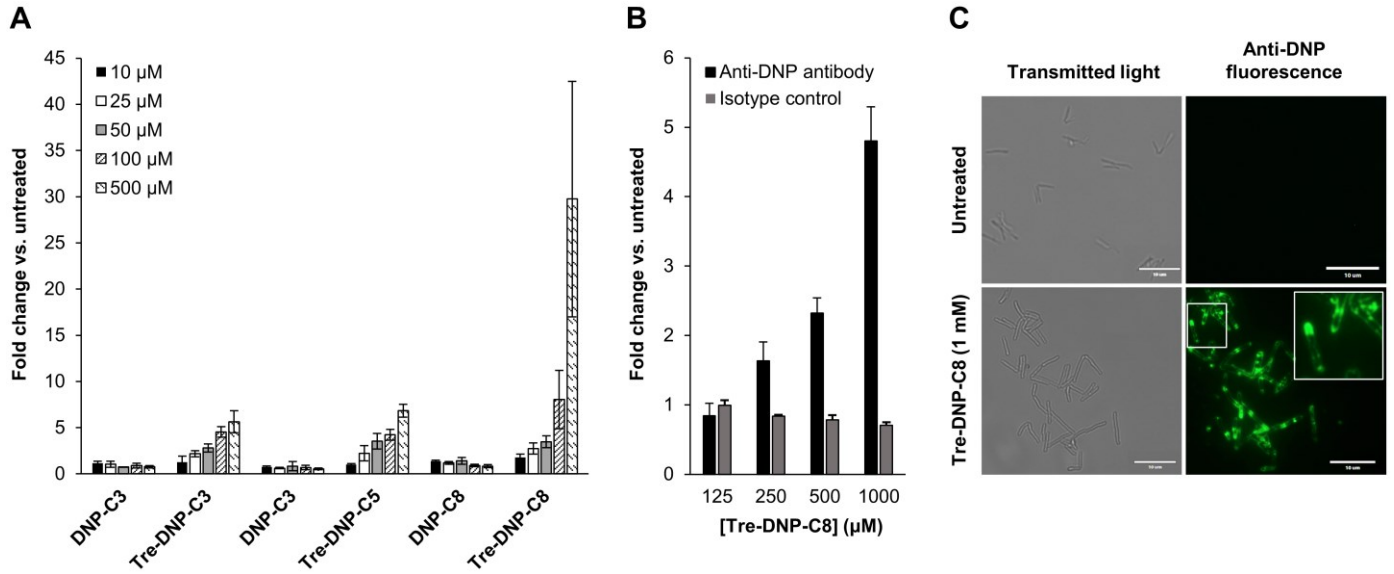

Figure 2. Tre-DNP analogues incorporate into the cell surface of *M. smegmatis*. Bacteria were incubated in Tre-DNP or DNP-carboxylic acid at the indicated concentration (or left untreated) for 16 h, washed, stained with fluorescent anti-DNP-KLH antibody (or isotype control for panel B), fixed, washed, and analyzed by (A and B) flow cytometry and (C) fluorescence microscopy. Error bars in panels A and B denote the standard deviation of three replicate experiments. Y-axes on plots in panels A and B are fold change in mean fluorescence intensity versus control cells that were not treated with compound but were subjected to the antibody staining step. Scale bars in panel C, 10 µm.

Given the initial results from the evaluation of compounds **1**–**3**, Tre-DNP-C8 (**3**) was selected for further evaluation. Tre-DNP-C8 did not impact the growth of *M. smegmatis* in 7H9 culture medium at concentrations up to 1 mM, suggesting that efficient DNP incorporation could be achieved without impairment of normal physiological functions (Figure S1, Supporting Information). Incorporation of Tre-DNP-C8 into *M. smegmatis* was found to be time-dependent, with maximum signal observed following incubation of bacteria with compound for 4–16 h (one doubling time is approximately 4 h for *M. smegmatis* grown in a 96-well plate) (Figure 3A). Additional experiments were performed to determine whether the incorporation of Tre-DNP-C8 was metabolically driven and dependent on trehalose metabolism. Although live *M. smegmatis* cells efficiently incorporated Tre-DNP-C8 into their cell surface, bacteria that were heat- or paraformaldehyde-killed did not incorporate the compound, demonstrating that metabolic activity was required for incorporation (Figure 3B). Competition experiments showed that Tre-DNP-C8 incorporation was diminished by the addition of exogenous native trehalose in a dose-dependent manner (Figure 3C), which, along with lack of incorporation observed for the trehalose-deficient DNP-carboxylic acids (Figure 2A), confirmed dependency of Tre-DNP-C8 incorporation on trehalose metabolism. Tre-DNP-C8 incorporation into *M. smegmatis* was also diminished by treatment with the mycoloyltransferase inhibitor ebselen (Figure 3D) and by partial knock-out of mycoloyltransferase activity (Figure 3E). These data are consistent with the proposed route of extracellular mycoloyltransferase-mediated incorporation into cell-surface glycolipids (Scheme S1, Supporting Information), but do not fully rule out other possible avenues of binding. It was also found that Tre-DNP-C8 incorporated efficiently into mycomembrane-containing *M. smegmatis* and *Corynebacterium glutamicum* but did not incorporate appreciably into Gram-negative *Escherichia coli* or Gram-positive *Bacillus subtilis* (Figure 3F). Finally, it was confirmed that Tre-DNP-C8 did not incorporate directly into mammalian THP-1 cells, supporting the notion that the trehalose targeting strategy would avoid modification of host cells (Figure S2, Supporting Information). Together, our data demonstrate that Tre-DNP-C8 efficiently and specifically installs DNP groups into cell surface glycolipids in *M. smegmatis* and other mycomembrane-containing bacteria.

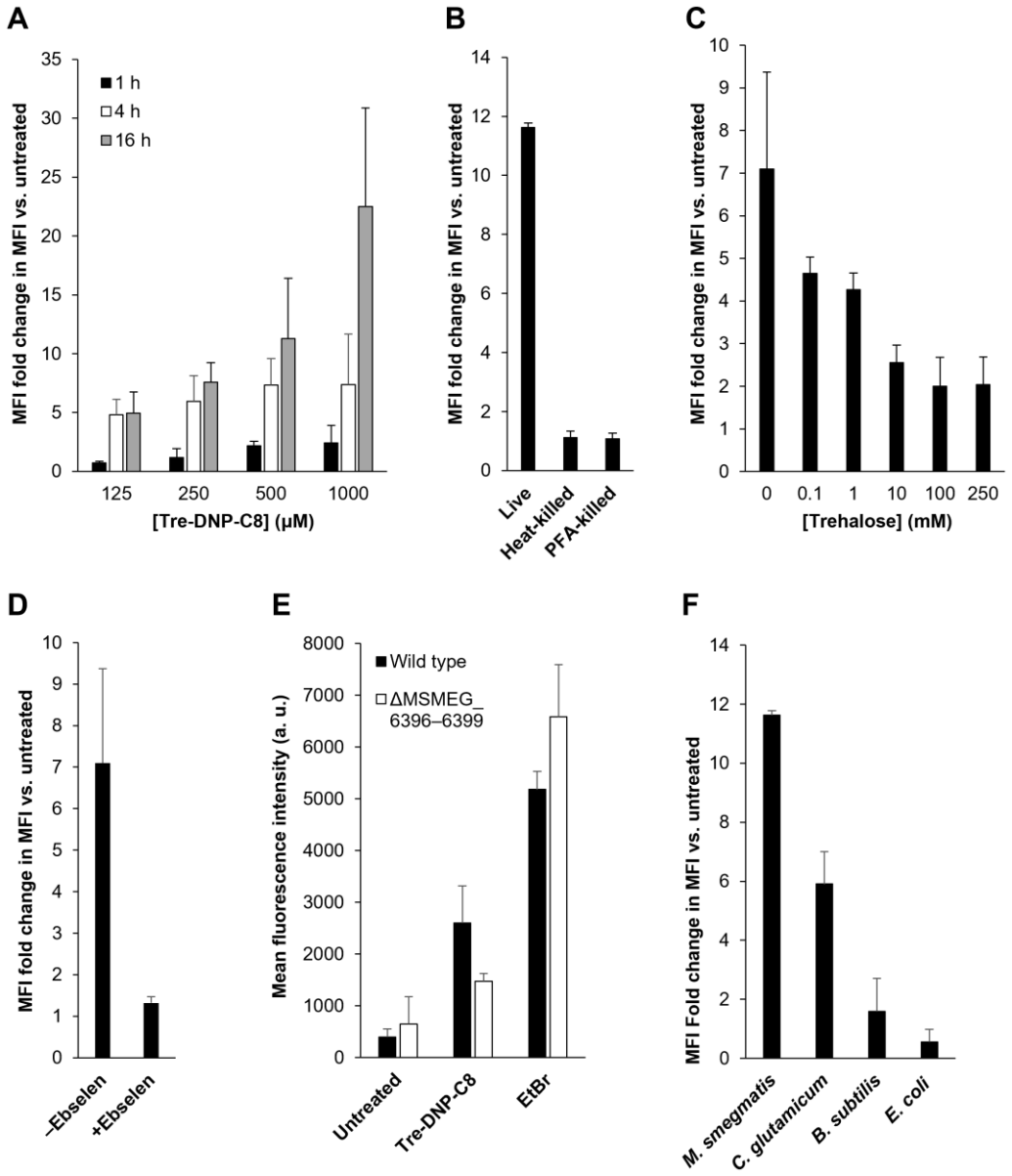

Figure 3. Tre-DNP-C8 specifically incorporates into *M. smegmatis* via trehalose metabolism. (A) *M. smegmatis* was incubated for 1–16 h with Tre-DNP-C8 at varying concentrations and times, or left untreated, then cells were washed, stained with fluorescent anti-DNP-KLH antibody, washed, fixed, and analyzed by flow cytometry. (B) Live, heat-killed, or paraformaldehyde-killed *M. smegmatis* were treated with Tre-DNP-C8 (250 μM), then processed and analyzed as in (A). (C) *M. smegmatis* was treated with Tre-DNP-C8 (250 μM) in varying concentrations of competing exogenous native trehalose, then processed and analyzed as in (A). (D) *M. smegmatis* was treated with Tre-DNP (250 μM) in the presence or absence of Ag85 inhibitor ebselen (100 μg/mL), then processed and analyzed as in (A). (E) *M. smegmatis* wild type or Ag85-deficient mutant Δ*MSMEG_6396–6399* were incubated with Tre-DNP-C8 (250 μM) or permeability control compound ethidium bromide (EtBr, 5 μg/mL), then processed and analyzed as in (A). (F) *M. smegmatis*, *C. glutamicum*, *B. subtilis*, or *E. coli* were treated with Tre-DNP-C8 (250 μM), then processed and analyzed as in (A). MFI, mean fluorescence intensity in arbitrary units (a.u.). Error bars denote the standard deviation of three replicate experiments.

Tre-DNP-C8 enhances phagocytosis of mycobacteria. Based on the findings that Tre-DNP-C8 specifically incorporates into mycobacteria and recruits anti-DNP antibodies to the mycobacterial surface, we

next investigated whether opsonization by anti-DNP antibodies enhanced phagocytosis of GFP-expressing *M. smegmatis*. For these experiments, we used unlabeled anti-DNP IgG as a source of opsonin, and we tested whether the percentage of THP-1 cells that engulfed Tre-DNP-C8-modified *M. smegmatis* increased relative to unmodified *M. smegmatis*. First, we confirmed that non-conjugated anti-DNP antibody bound to *M. smegmatis* displaying Tre-DNP-C8 by using a fluorescent secondary antibody (anti-mouse IgG PE, Figure 4A). Next, using adapted literature procedures,[58–61] phorbol 12-myristate 13-acetate (PMA)-differentiated THP-1 cells were co-cultured with Tre-DNP-C8-labeled, anti-DNP antibody-opsonized *M. smegmatis*, then harvested and fixed. Antibody opsonization was performed before co-culture to minimize non-specific binding to THP-1 cells and flow cytometry was used to measure the percentage of THP-1 cells that engulfed *M. smegmatis* (Figures 4B-C). On average, 13.4% of THP-1 cells engulfed unmodified *M. smegmatis*, establishing a baseline level of phagocytosis. Pre-incubation of anti-DNP antibodies with unmodified *M. smegmatis* did not increase engulfment whatsoever, but Tre-DNP-C8 labeling without anti-DNP opsonization increased phagocytosis modestly to 17.8%. In contrast to this modest increase resulting from Tre-DNP-C8 labeling, 30.0% of THP-1 cells engulfed opsonized, Tre-DNP-C8-modified *M. smegmatis*. Given that there was little to no increase in the percentage of THP-1 cells that engulfed non-opsonized or unmodified *M. smegmatis*, these data suggest that DNP modification and anti-DNP antibody opsonization are necessary for enhanced uptake by THP-1 cells. These data demonstrate for the first time that the ARM immune-targeting strategy can be extended to mycobacteria by leveraging mycobacteria-specific trehalose–DNP conjugates.

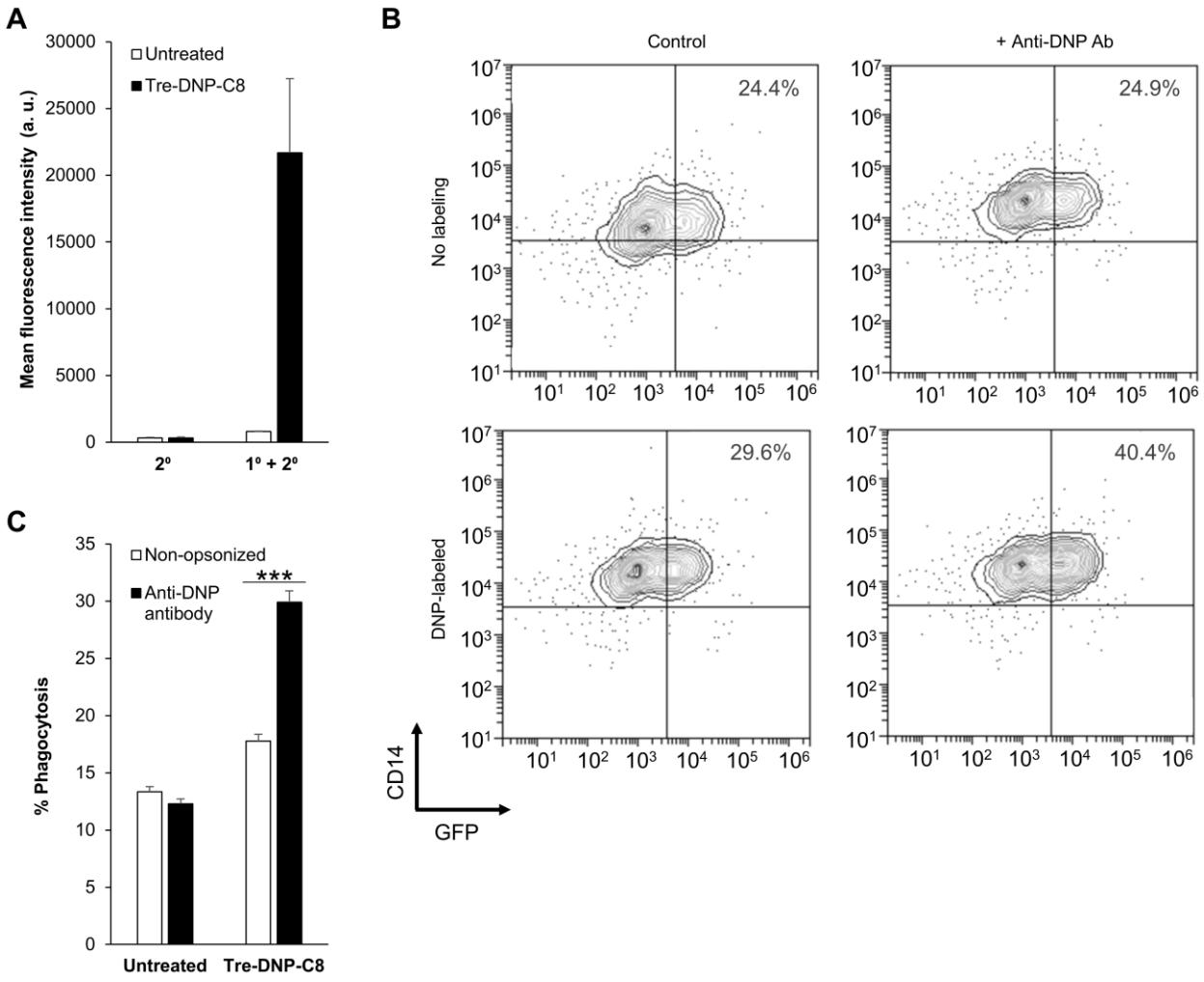

Figure 4. Tre-DNP-C8 enhances phagocytosis of *M. smegmatis* by THP-1 cells. (A) Anti-DNP antibody binding to Tre-DNP-C8-labeled *M. smegmatis*. GFP-expressing *M. smegmatis* was cultured in the presence or absence of Tre-DNP-C8 (250 μM), washed, stained with primary mouse anti-DNP IgG antibodies (1º) followed by secondary PE-conjugated anti-mouse IgG antibodies (2º), and analyzed by flow cytometry. The Y-axis shows the mean fluorescence intensity and error bars denote the standard deviation of three replicate experiments. (B-C) Tre-DNP-C8-modified and -unmodified GFP-expressing *M. smegmatis* were treated with or without anti-DNP antibody, then bacteria (1 x 10^6 CFU/mL) were co-cultured with PMA-differentiated THP-1 cells (1 x 10^6 cells/mL). Phagocytosis was analyzed by flow cytometry (B) and calculated as: $CD14^+GFP^+$ cells/total $CD14^+$cells x 100% (C). Error bars in (C) denote standard deviation of 4 independent experiments. Statistical analysis was conducted using two-way ANOVA Sidak's multiple comparison test (*** $p \leq 0.001$).

Conclusion

Given the enormous global health burden presented by mycobacterial diseases and the challenge in treating these diseases with traditional chemotherapies, there is an urgent need to develop alternative treatment strategies, such as immunotherapies. In this study, we developed a strategy to specifically engineer mycobacterial surface glycans with the hapten DNP using trehalose as the targeting moiety, which was demonstrated to augment the immune response to mycobacteria, specifically enhancement of phagocytosis.

Our work extends prior studies that exploited trehalose conjugation to deliver therapeutic cargo to mycobacteria, including drug-loaded nanoparticles and photosensitizers,[50,62] thus further validating this approach to targeting mycobacteria. Having now established proof-of-concept for the first ARM-based immune targeting strategy for mycobacteria, we envision several future directions. As the current work focused on the avirulent model organism *M. smegmatis*, we aim to evaluate Tre-DNP ARMs for their ability to enhance phagocytosis and killing of pathogenic mycobacteria, including NTM species and *M. tuberculosis*. Antibody-mediated signaling can restrict the growth of intracellular pathogens,[20–25] but outcomes associated with antibody-mediated phagocytosis of mycobacteria have been variable.[19] Using DNP as the surface antigen may help to overcome issues related to antigenic determinants and immune evasion, and, furthermore, will enable us to quantify how antibodies affect macrophage intracellular killing, cytokine production, and their polarization state.[29] With respect to improving the ARM strategy, we plan to optimize the efficiency of DNP surface display for different mycobacterial organisms by tuning the trehalose conjugate linker type and length (including linkers designed for improved metabolic stability), which we have previously shown can impact incorporation efficiency and mechanism.[49,55] Furthermore, we will explore ARM delivery to mycobacteria using two-step bioorthogonal approaches, such as strain-promoted azide–alkyne cycloaddition[63] or tetrazine ligation[64] employing our reported azide- and *trans*-cyclooctene-modified trehalose derivatives, respectively.[49,54] Another area of future investigation is to consider the potential effect of surface modification on native glycolipid-dependent immunoactivity, although it is noted that only a fraction of the native surface glycolipids are replaced with DNP-modified forms in this strategy. In addition to the continued development and investigation of our mycobacteria-specific ARM strategy and evaluating its future potential as an immunotherapy against pathogens, we envision that it will be useful as a tool for investigating host–pathogen interactions, namely helping to elucidate the roles of antibodies in the immune response to mycobacterial infections.

Methods

Bacterial strains and growth conditions. The bacterial strains used in this work included *M. smegmatis* mc^{2}155 wild type, *M. smegmatis* ΔMSMEG_6396–6399,[53] *C. glutamicum* 534, *Escherichia coli* K12 MG1655, and *Bacillus subtilis* 168. *M. smegmatis* strains were cultured in Middlebrook 7H9 liquid medium supplemented with ADC (albumin, dextrose, and catalase), 0.5% glycerol, and 0.05% Tween-80. *C. glutamicum*, *E. coli*, and

B. subtilis were cultured in LB liquid medium. All bacteria were cultured at 37 °C, except *C. glutamicum*, which was cultured at 30 °C.

Tre-DNP incorporation experiments. Bacterial starter culture was generated by inoculating a single colony from a freshly streaked LB or 7H10 agar plate into 3 mL liquid 7H9 medium in a culture tube. The starter culture was incubated at 37 °C (or 30 °C for *C. glutamicum*) with shaking until reaching mid-logarithmic phase and then diluted with liquid medium to the desired density for initiating experiments. Evaluation of Tre-DNP incorporation and growth effects was performed in triplicate in sterile flat-bottom 96-well plates. First, starter culture was diluted with 7H9 liquid medium to a final optical density at 600 nm (OD_{600}) of 0.2. Cells were mixed with DNP-carboxylic acid or Tre-DNP stock solutions (both prepared in H_2O), or 7H9 medium for untreated controls, to achieve the desired compound concentration (0–1 mM) and a final volume of 200 µL. The plate was incubated at 37 °C with shaking in a microplate reader (Tecan Infinite F200 or M200 PRO operated by Tecan iControl software) for 1–16 h. In growth evaluation experiments, absorbance at 600 nm (OD_{600}) was measured periodically to construct growth curves. Following the Tre-DNP incubation step, well contents were transferred to a v-bottom 96-well plate and the cells were centrifuged (3,200 xg, 5 min, room temperature) and washed with 1x phosphate-buffered saline containing 0.5% BSA (PBS-B) three times. To each well, 1 µL of 2 mg/mL anti-dinitrophenyl-KLH Alexa Flour 488 conjugate (or 1 µL of 100 µg/mL IgG isotype control, Alexa Fluor 488 conjugate) was added, and the plate was left for 60 min in the dark without being disturbed. Cells were then fixed in 4% paraformaldehyde in PBS (180 µL) for 20 min at room temperature. Fixed cells were centrifuged and washed with PBS-B three times as described above, re-suspended in 100 µL of PBS, then analyzed by flow cytometry and/or fluorescence microscopy as described in the supplementary methods.

The same general procedure described above was used for all Tre-DNP incorporation experiments with the following modifications. For the heat-kill control experiment, *M. smegmatis* cells were heat-killed by heating at 95 °C for 30 min prior to the Tre-DNP incorporation procedure. For the paraformaldehyde fixation control experiment, *M. smegmatis* cells were fixed by treatment with 4% paraformaldehyde in PBS (180 µL) for 20 min at room temperature prior to the Tre-DNP incorporation procedure. For the trehalose competition experiment, *M. smegmatis* cells were co-treated with Tre-DNP analogue and varying concentrations of trehalose (0–250 mM) during the incubation step, followed by processing as described above. For the ebselen inhibition experiment, *M. smegmatis* cells were incubated for 3 h with and without ebselen (100 µg/mL), followed by treatment with Tre-

DNP-C8 Treatment and processing as described above. For the mycoloyltransferase mutant experiment, *M. smegmatis* wild type (WT) and *M. smegmatis* mutant*, ΔMSMEG_6396–6399* were treated with Tre-DNP-8C, ethidium bromide (EtBr, permeability control compound, 5 μg/mL), or left untreated and processed as described above. Cells were analyzed by flow cytometry and/or fluorescence microscopy as described in the Supporting Information.

***Opsonization with unlabeled anti-DNP antibodies*.** To opsonize unmodified and Tre-DNP-C8-labeled *M. smegmatis*, 2 x 10^6 CFU/mL of bacteria were incubated with 1 μg/100 μL of monoclonal mouse anti-DNP IgG (Millipore) for 1 h at 37 °C. To confirm opsonization, bacteria were washed three times with PBS-B and stained with 0.2 μg/100 μL anti-mouse IgG-PE for 30 min at 37 °C in the dark. Cells were washed three times with PBS-B, fixed, and analyzed by flow cytometry.

***Phagocytosis of* M. smegmatis.** THP-1 cells were purchased from ATCC. Cells were maintained between 2 x 10^5 and 10 x 10^5 cells/ml in RPMI I640 (Gibco) supplemented with 10% heat-inactivated fetal bovine serum, 0.05 mM 2-mercaptoethanol, 1% penicillin/streptomycin and incubated at 37 °C and in 5% CO_2. Cells were used between passage numbers 5 and 20. THP-1 cells were seeded in complete media at 1x10^6 cells/mL into 12-well treated tissue culture plates and differentiated with 100 nM phorbol 12-myristate 13-acetate (PMA) in complete media for 16 h in 5% CO_2 at 37 °C. Media was replaced, and cells were allowed to rest for 48 h. GFP-expressing *M. smegmatis* were either left alone or modified with Tre-DNP-C8, and then subjected to mock treatment or antibody opsonization with anti-DNP IgG, as described above. Bacteria were washed, resuspended in phagocytosis buffer (5 mM $CaCl_2$ in RPMI), and co-cultured with THP-1 cells at a multiplicity of infection of infection of 1:1. To synchronize phagocytosis, cells were centrifuged at 1,600 rpm for 5 min at 4 °C, and allowed to incubate for 1 h. Subsequently, cells were washed three times with 1 mL RPMI and harvested by trypsinization. Cells were washed in FACS buffer (1% BSA in PBS), stained with 5 μL of anti-human CD14-APC (BioLegend) per million cells for 20 mins and washed. After the third wash, cells were treated with 45 μg/mL of bromophenol blue in FACS to quench fluorescence of extracellular bacteria. Cells were again washed three times, resuspended in 200 μL of PBS and flow cytometry was conducted immediately to determine percentage phagocytosis.

The Supporting Information contains supplementary figures, methods, and NMR spectra. This material is

available free of charge via the internet at http://pubs.acs.org.

Acknowledgements

This work was supported by grants to B.M.S. from the National Institutes of Health (R15 AI117670) and to M. C. G-W. from the National Institutes of Health (R15 GM132992). NMR instrumentation was supported by NSF MRI Award 2117338 (B.M.S.).

References

(1) World Health Organization. *Global Tuberculosis Report*, **2022**.

(2) Reid, M. J. A.; Arinaminpathy, N.; Bloom, A.; Bloom, B. R.; Boehme, C.; Chaisson, R.; Chin, D. P.; Churchyard, G.; Cox, H.; Ditiu, L.; Dybul, M.; Farrar, J.; Fauci, A. S.; Fekadu, E.; Fujiwara, P. I.; Hallett, T. B.; Hanson, C. L.; Harrington, M.; Herbert, N.; Hopewell, P. C.; Ikeda, C.; Jamison, D. T.; Khan, A. J.; Koek, I.; Krishnan, N.; Motsoaledi, A.; Pai, M.; Raviglione, M. C.; Sharman, A.; Small, P. M.; Swaminathan, S.; Temesgen, Z.; Vassall, A.; Venkatesan, N.; van Weezenbeek, K.; Yamey, G.; Agins, B. D.; Alexandru, S.; Andrews, J. R.; Beyeler, N.; Bivol, S.; Brigden, G.; Cattamanchi, A.; Cazabon, D.; Crudu, V.; Daftary, A.; Dewan, P.; Doepel, L. K.; Eisinger, R. W.; Fan, V.; Fewer, S.; Furin, J.; Goldhaber-Fiebert, J. D.; Gomez, G. B.; Graham, S. M.; Gupta, D.; Kamene, M.; Khaparde, S.; Mailu, E. W.; Masini, E. O.; McHugh, L.; Mitchell, E.; Moon, S.; Osberg, M.; Pande, T.; Prince, L.; Rade, K.; Rao, R.; Remme, M.; Seddon, J. A.; Selwyn, C.; Shete, P.; Sachdeva, K. S.; Stallworthy, G.; Vesga, J. F.; Vilc, V.; Goosby, E. P. Building a Tuberculosis-Free World: The Lancet Commission on Tuberculosis. *The Lancet*. **2019**, *393* (10178), 1331–1384.

(3) Boldrin, F.; Provvedi, R.; Mazzabò, L. C.; Segafreddo, G.; Manganelli, R. Tolerance and Persistence to Drugs: A Main Challenge in the Fight Against *Mycobacterium tuberculosis*. *Front. Microbiol.* **2020**, *11*, 1924.

(4) Lacobino, A.; Fattorini, L.; Giannoni, F. Drug-Resistant Tuberculosis 2020: Where We Stand. *Appl. Sci.* **2020**, *10* (6), 2153.

(5) Marahatta, S. B. Multi-Drug Resistant Tuberculosis Burden and Risk Factors: An Update. *Kathmandu Univ. Med. J.* **2010**, *8* (1), 116–125.

(6) Winthrop, K. L.; Marras, T. K.; Adjemian, J.; Zhang, H.; Wang, P.; Zhang, Q. Incidence and Prevalence of Nontuberculous Mycobacterial Lung Disease in a Large U . S. Managed Care Health Plan, 2008 – 2015. *AnnalsATS* **2020**, *17* (2), 2008–2015.

(7) Diel, R.; Jacob, J.; Lampenius, N.; Loebinger, M.; Nienhaus, A.; Rabe, K. F.; Ringshausen, F. C. Burden of Non-Tuberculous Mycobacterial Pulmonary Disease in Germany. *Eur. Respir. J.* **2017**, *49* (4), 1602109.

(8) Chen, J.; Zhao, L.; Mao, Y.; Ye, M.; Guo, Q.; Zhang, Y.; Xu, L.; Zhang, Z.; Li, B.; Chu, H. Clinical Efficacy and Adverse Effects of Antibiotics Used to Treat Mycobacterium Abscessus Pulmonary Disease. *Front. Microbiol.* **2019**, *10*, 1977.

(9) Griffith, D. E.; Aksamit, T.; Brown-Elliott, B. A.; Catanzaro, A.; Daley, C.; Gordin, F.; Holland, S. M.; Horsburgh, R.; Huitt, G.; Iademarco, M. F.; Iseman, M.; Olivier, K.; Ruoss, S.; von Reyn, C. F.; Wallace,

R. J.; Winthrop, K. An Official ATS/IDSA Statement: Diagnosis, Treatment, and Prevention of Nontuberculous Mycobacterial Diseases. *Am. J. Respir. Crit. Care Med.* **2007**, *175* (4), 367–416.

(10) Forbes, B. A.; Hall, G. S.; Miller, M. B.; Novak, S. M.; Rowlinson, M.-C.; Salfinger, M.; Somoskövi, A.; Warshauer, D. M.; Wilson, M. L. Practical Guidelines for Clinical Microbiology Laboratories: Mycobacteria. **2018,** *32* (2), e00038-17.

(11) Aslam, B.; Wang, W.; Arshad, M. I.; Khurshid, M.; Muzammil, S.; Rasool, M. H.; Nisar, M. A.; Alvi, R. F.; Aslam, M. A.; Qamar, M. U.; Salamat, M. K. F.; Baloch, Z. Antibiotic Resistance: A Rundown of a Global Crisis. *Infect. Drug Resist.* **2018**, *11*, 1645–1658.

(12) Wu, M. L.; Aziz, D. B.; Dartois, V.; Dick, T. NTM Drug Discovery: Status, Gaps and the Way Forward. *Drug Discov. Today*. **2018**, *23* (8), 1502–1519.

(13) Kilinç, G.; Saris, A.; Ottenhoff, T. H. M.; Haks, M. C. Host-Directed Therapy to Combat Mycobacterial Infections. *Immunol. Rev.* **2021**, *301* (1), 62–83.

(14) Poerio, N.; Riva, C.; Olimpieri, T.; Rossi, M.; Lorè, N. I.; de Santis, F.; de Angelis, L. H.; Ciciriello, F.; D'andrea, M. M.; Lucidi, V.; Cirillo, D. M.; Fraziano, M. Combined Host-and Pathogen-Directed Therapy for the Control of *Mycobacterium abscessus* Infection. *Microbiol. Spectr.* **2022**, *10*, e0254621.

(15) Jeong, E.-K.; Lee, H.-J.; Jung, Y.-J. Host-Directed Therapies for Tuberculosis. *Pathogens* **2022**, *11* (11), 1291.

(16) Kaufmann, S. H. E.; Dorhoi, A.; Hotchkiss, R. S.; Bartenschlager, R. Host-Directed Therapies for Bacterial and Viral Infections. *Nat. Rev. Drug Discov.* **2018**, *17* (1), 35–56.

(17) Nunes-Alves, C.; Booty, M. G.; Carpenter, S. M.; Jayaraman, P.; Rothchild, A. C.; Behar, S. M. In Search of a New Paradigm for Protective Immunity to TB. *Nat. Rev. Microbiol.* **2014**, *12* (4), 289–299.

(18) Ratnatunga, C. N.; Lutzky, V. P.; Kupz, A.; Doolan, D. L.; Reid, D. W.; Field, M.; Bell, S. C.; Thomson, R. M.; Miles, J. J. The Rise of Non-Tuberculosis Mycobacterial Lung Disease. *Front. Immunol.* **2020,** *11*, 303.

(19) Li, H.; Javid, B. Antibodies and Tuberculosis: Finally Coming of Age? *Nat. Rev. Immunol.* **2018**, *18* (9), 591–596.

(20) Watson, A.; Li, H.; Ma, B.; Weiss, R.; Bendayan, D.; Abramovitz, L.; Ben-Shalom, N.; Mor, M.; Pinko, E.; Bar Oz, M.; Wang, Z.; Du, F.; Lu, Y.; Rybniker, J.; Dahan, R.; Huang, H.; Barkan, D.; Xiang, Y.; Javid, B.; Freund, N. T. Human Antibodies Targeting a Mycobacterium Transporter Protein Mediate Protection against Tuberculosis. *Nat. Commun.* **2021**, *12*, 602.

(21) Lausen, M.; Pedersen, M. S.; Kader Rahman, N. S.; Holm-Nielsen, L. T.; Farah, F. Y. M.; Christiansen, G.; Birkelund, S. Opsonophagocytosis of Chlamydia Pneumoniae by Human Monocytes and Neutrophils. *Infect. Immun.* **2020**, *88* (7), e00087-20.

(22) Geier, H.; Celli, J. Phagocytic Receptors Dictate Phagosomal Escape and Intracellular Proliferation of Francisella Tularensis. *Infect. Immun.* **2011**, *79* (6), 2204–2214.

(23) Joller, N.; Weber, S. S.; Oxenius, A. Antibody – Fc Receptor Interactions in Protection against Intracellular Pathogens. *Eur. J. Immunol.* **2011**, 889–897.

(24) Bournazos, S.; Gupta, A.; Ravetch, J. v. The Role of IgG Fc Receptors in Antibody-Dependent Enhancement. *Nat. Rev. Immunol.* **2020**, *20* (10), 633–643.

(25) Joller, N.; Weber, S. S.; Müller, A. J.; Spörri, R.; Selchow, P.; Sander, P.; Hilbi, H.; Oxenius, A. Antibodies Protect against Intracellular Bacteria by Fc Receptor-Mediated Lysosomal Targeting. *Proc. Natl. Acad. Sci. U.S.A.* **2010**, *107* (47), 20441–20446.

(26) Spiegel, D. A. A Call to ARMs: The Promise of Immunomodulatory Small Molecules. *Expert Rev. Clin. Pharmacol.* **2013**, *6* (3), 223–225.

(27) McEnaney, P. J.; Parker, C. G.; Zhang, A. X. Antibody-Recruiting Small Molecules: Synthetic Constructs as Immunotherapeutics. *Annu. Rep. Med. Chem.* **2017**, *50*, 481–518.

(28) McEnaney, P. J.; Parker, C. G.; Zhang, A. X.; Spiegel, D. A. Antibody-Recruiting Molecules: An Emerging Paradigm for Engaging Immune Function in Treating Human Disease. *ACS Chem. Biol.* **2012**, *7* (7), 1139–1151.

(29) Charles, W. Z.; Faries, C. R.; Street, Y. T.; Flowers, L. S.; McNaughton, B. R. Antibody-Recruitment as a Therapeutic Strategy: A Brief History and Recent Advances. *ChemBioChem*. **2022**, *23* (16), e202200092.

(30) Uvyn, A.; de Geest, B. G. Multivalent Antibody-Recruiting Macromolecules: Linking Increased Binding Affinity with Enhanced Innate Immune Killing. *ChemBioChem*. **2020**, *21* (21), 3036–3043.

(31) Jakobsche, C. E.; Mcenaney, P. J.; Zhang, A. X.; Spiegel, D. A.; Chem, A.; Author, B. Reprogramming Urokinase into an Antibody-Recruiting Anticancer Agent. *ACS Chem. Biol.* **2012**, *7* (2), 316–321.

(32) Murelli, R. P.; Zhang, A. X.; Michel, J.; Jorgensen, W. L.; Spiegel, D. A. Chemical Control over Immune Recognition: A Class of Antibody-Recruiting Small Molecules That Target Prostate Cancer. *J. Am. Chem. Soc.* **2009**, *131* (47), 17090–17092.

(33) Rullo, A. F.; Fitzgerald, K. J.; Muthusamy, V.; Liu, M.; Yuan, C.; Huang, M.; Kim, M.; Cho, A. E.; Spiegel, D. A. Re-Engineering the Immune Response to Metastatic Cancer: Antibody-Recruiting Small Molecules Targeting the Urokinase Receptor. *Angew. Chem. Int. Edit.* **2016**, *55* (11), 3642–3646.

(34) Uvyn, A.; de Coen, R.; de Wever, O.; Deswarte, K.; Lambrecht, B. N.; de Geest, B. G. Cell Surface Clicking of Antibody-Recruiting Polymers to Metabolically Azide-Labeled Cancer Cells. *Chem. Commun.* **2019**, *55* (73), 10952–10955.

(35) Parker, C. G.; Domaoal, R. A.; Anderson, K. S.; Spiegel, D. A. An Antibody-Recruiting Small Molecule That Targets HIV Gp120. *J. Am. Chem. Soc.* **2009**, *131* (45), 16392–16394.

(36) Chirkin, E.; Muthusamy, V.; Mann, P.; Roemer, T.; Nantermet, P. G.; Spiegel, D. A. Neutralization of Pathogenic Fungi with Small-Molecule Immunotherapeutics. *Angew. Chem. Int. Edit.* **2017**, *129* (42), 13216–13220.

(37) Fura, J. M.; Sabulski, M. J.; Pires, M. M. D-Amino Acid Mediated Recruitment of Endogenous Antibodies to Bacterial Surfaces. *ACS Chem. Biol.* **2014**, *9* (7), 1480–1489.

(38) Idso, M. N.; Akhade, A. S.; Arrieta-Ortiz, M. L.; Lai, B. T.; Srinivas, V.; Hopkins, J. P.; Gomes, A. O.; Subramanian, N.; Baliga, N.; Heath, J. R. Antibody-Recruiting Protein-Catalyzed Capture Agents to Combat Antibiotic-Resistant Bacteria. *Chem. Sci.* **2020**, *11* (11), 3054–3067.

(39) Sabulski, M. J.; Pidgeon, S. E.; Pires, M. M. Immuno-Targeting of Staphylococcus Aureus via Surface Remodeling Complexes. *Chem. Sci.* **2017**, *8* (10), 6804–6809.

(40) Kaewsapsak, Pornchai; Esonu, Onyinyechi; Dube, D. H. Recruiting the Host's Immune System To Target Helicobacter Pylori's Surface Glycans. *ChemBioChem.* **2013**, *14* (6), 721–726.

(41) Dalesandro, B. E.; Pires, M. M. Induction of Endogenous Antibody Recruitment to the Surface of the Pathogen *Enterococcus faecium*. *ACS Infect. Dis.* **2021**, *7* (5), 1116–1125.

(42) Hyun, J. Y.; Lee, C. H.; Lee, H.; Jang, W. D.; Shin, I. Bacterial Lectin-Targeting Glycoconjugates for Selective Elimination of Pathogenic Bacteria. *ACS Macro Lett.* **2020**, *9* (10), 1429–1432.

(43) Jakobsche, C. E.; Parker, C. G.; Tao, R. N.; Kolesnikova, M. D.; Douglass, E. F.; Spiegel, D. A. Exploring Binding and Effector Functions of Natural Human Antibodies Using Synthetic Immunomodulators. *ACS Chem. Biol.* **2013**, *8* (11), 2404–2411.

(44) Ortega, E.; Kostovetzky, M.; Larralde, C. Natural DNP-Binding Immunoglobulins and Antibody Multispecificity. *Mol. Immunol.* **1984**, *21* (10), 883–888.

(45) O'Neill, M. K.; Piligian, B. F.; Olson, C. D.; Woodruff, P. J.; Swarts, B. M. Tailoring Trehalose for Biomedical and Biotechnological Applications. *Pure Appl. Chem.* **2017**, *89*, 1223–1249.

(46) Dulberger, C. L.; Rubin, E. J.; Boutte, C. C. The Mycobacterial Cell Envelope — a Moving Target. *Nat. Rev. Microbiol.* **2020**, 18 (1), 47–59.

(47) Angala, S. K.; Belardinelli, J. M.; Huc-Claustre, E.; Wheat, W. H.; Jackson, M. The Cell Envelope Glycoconjugates of *Mycobacterium tuberculosis*. *Crit. Rev. Biochem. Mol. Biol.* **2014**, *49* (5), 361–399.

(48) Backus, K. M.; Boshoff, H.; Barry, C. S.; Boutureira, O.; Patel, M. K.; D'Hooge, F.; Lee, S. S., Via, L. E.; Tahlan, K.; Barry III, C. E.; Davis, B. G. Uptake of Unnatural Trehalose Analogs as a Reporter for *Mycobacterium tuberculosis*. *Nat. Chem. Biol.* **2011**, *7*, 228–235.

(49) Fiolek, T. J.; Banahene, N.; Kavunja, H. W.; Holmes, N. J.; Rylski, A. K.; Pohane, A. A.; Siegrist, M. S.; Swarts, B. M. Engineering the Mycomembrane of Live Mycobacteria with an Expanded Set of Trehalose Monomycolate Analogues. *ChemBioChem.* **2019**, *20* (10), 1282–1291.

(50) Dutta, A. K.; Choudhary, E.; Wang, X.; Záhorszka, M.; Forbak, M.; Lohner, P.; Jessen, H. J.; Agarwal, N.; Kordulákova, J.; Jessen-Trefzer, C. Trehalose Conjugation Enhances Toxicity of Photosensitizers against Mycobacteria. *ACS Cent. Sci.* **2019**, *5* (4), 644–650.

(51) Banahene, N.; Gepford, D. M.; Biegas, K. J.; Swanson, D. H.; Hsu, Y. P.; Murphy, B. A.; Taylor, Z. E.; Lepori, I.; Siegrist, M. S.; Obregón-Henao, A.; van Nieuwenhze, M. S.; Swarts, B. M. A Far-Red Molecular Rotor Fluorogenic Trehalose Probe for Live Mycobacteria Detection and Drug-Susceptibility Testing. *Angew. Chem. Int. Edit.* **2023**, *62* (2), e202213563.

(52) Rundell, S. R.; Wagar, Z. L.; Meints, L. M.; Olson, C. D.; O'Neill, M. K.; Piligian, B. F.; Poston, A. W.; Hood, R. J.; Woodruff, P. J.; Swarts, B. M. Deoxyfluoro-D-Trehalose (FDTre) Analogues as Potential PET Probes for Imaging Mycobacterial Infection: Rapid Synthesis and Purification, Conformational Analysis, and Uptake by Mycobacteria. *Org. Biomol. Chem.* **2016**, 8698–8609.

(53) Kamariza, M.; Shieh, P.; Ealand, C. S.; Peters, J. S.; Chu, B.; Rodriguez-Rivera, F. P.; Babu Sait, M. R.; Treuren, W. v.; Martinson, N.; Kalscheuer, R.; Kana, B. D.; Bertozzi, C. R. Rapid Detection of *Mycobacterium tuberculosis* in Sputum with a Solvatochromic Trehalose Probe. *Sci. Transl. Med.* **2018**, *10* (430), eaam6310.

(54) Swarts, B. M.; Holsclaw, C. M.; Jewett, J. C.; Alber, M.; Fox, D. M.; Siegrist, M. S.; Leary, J. A.; Kalscheuer, R.; Bertozzi, C. R. Probing the Mycobacterial Trehalome with Bioorthogonal Chemistry. *J. Am. Chem. Soc.* **2012**, *134* (39), 16123–16126.

(55) Foley, H. N.; Stewart, J. A.; Kavunja, H. W.; Rundell, S. R.; Swarts, B. M. Bioorthogonal Chemical Reporters for Selective in Situ Probing of Mycomembrane Components in Mycobacteria. *Angew. Chem. Int. Edit.* **2016**, *55* (6), 2053–2057.

(56) Sarpe, V. A.; Kulkarni, S. S. Synthesis of Maradolipid. *J. Org. Chem.* **2011**, *76* (16), 6866–6870.

(57) Seela, F.; Hansska, F.; Watanabe, K.; Cramer, F. Introduction of Antigenic Determining 2,4-Dinitrophenyl Residues into 4-Thiouridine. *Nucleic Acids Res.* **1977**, *4* (3), 711-722.

(58) Sampaio, E. P.; Elloumi, H. Z.; Zelazny, A.; Ding, L.; Paulson, M. L.; Sher, A.; Bafica, A. L.; Shea, Y. R.; Holland, S. M. Mycobacterium Abscessus and M. Avium Trigger Toll-like Receptor 2 and Distinct Cytokine Response in Human Cells. *J. Respir. Cell Mol.* **2008**, *39* (4), 431–439.

(59) Lund, M. E.; To, J.; O'Brien, B. A.; Donnelly, S. The Choice of Phorbol 12-Myristate 13-Acetate Differentiation Protocol Influences the Response of THP-1 Macrophages to a pro-Inflammatory Stimulus. *J. Immunol. Methods* **2016**, *430*, 64–70.

(60) Hostetter, J.; Kagan, R.; Steadham, E. Opsonization Effects on Mycobacterium Avium Subsp. Paratuberculosis- Macrophage Interactions. *Clin. Diagn. Lab. Immunol.* **2005**, *12* (6), 793–796.

(61) Nuutila, J.; Lilius, E. M. Flow Cytometric Quantitative Determination of Ingestion by Phagocytes Needs the Distinguishing of Overlapping Populations of Binding and Ingesting Cells. *Cytometry A.* **2005**, *65* (2), 93–102.

(62) Zhou, J.; Jayawardana, K. W.; Kong, N.; Ren, Y.; Hao, N.; Yan, M.; Ramström, O. Trehalose-Conjugated, Photofunctionalized Mesoporous Silica Nanoparticles for Efficient Delivery of Isoniazid into Mycobacteria. *ACS Biomater. Sci. Eng.* **2015**, *1* (12), 1250–1255.

(63) Jewett, J. C.; Bertozzi, C. R. Cu-Free Click Cycloaddition Reactions in Chemical Biology. *Chem. Soc. Rev.* **2010**, *39 (4)*, 1272–1279.

(64) Blackman, M. L.; Royzen, M.; Fox, J. M. Tetrazine Ligation: Fast Bioconjugation Based on Inverse-Electron-Demand Diels-Alder Reactivity. *J. Am. Chem. Soc.* **2008**, *130* (41), 13518–13519.

TOC Graphic